

Investigation of the characteristics of an intense ion beam propagated outside the diode

A.V. Stepanov^{1,*}, I.N. Pyatkov¹, Shijian Zhang², E.N. Stepanova¹

¹National Research Tomsk Polytechnic University, Tomsk, Russia

²School of Physics, Beihang University, Beijing, China

*stepanovav@mail.ru

Abstract. The characteristics of the high intense pulsed ion beam with energy up to 330 keV have been studied. The ion beam was extracted in the metal drift tube made in form of a cone. It was found that the metal tube provided the beam space charge neutralization up to 90% and increase in the beam current and energy density. The focusing factor of a beam current in the metal tube increased from 4.5 to 13. The mass ratio of ions propagated in the tube and in outer space had been varied. In this case, the proportion of protons in the tube increased from 75.7% to 84.7%.

Keywords: ion beam, drift tube, characteristics, space charge neutralization, focusing.

1. Introduction

Geometric focusing has been realized in the intense ion diodes of different types [1–6] for the formation and transportation of ion beams. This allows increasing the densities of the current and energy of the ion beam in the focus area by several times. However, the level of geometric focusing of the beam is limited due to the ion divergence [7]. The main factors that impact the ion divergence outside the diode system are the uncompensated current and the positive space charge of the ion beam [8, 9]. The positive space-charge creates intense electric fields, under the influence of which the ions deflect from the ideal trajectory. The result of the ion divergence is an increase the phase space of the beam and an inhomogeneous current and energy distribution in a beam cross section [8, 10]. In diodes with an external magnetic isolation, the coefficient of geometric focusing usually does not exceed 4–5 [11].

The various approaches to the transportation of intense pulsed ion beams with energy from several tens to hundreds of kiloelectron-volts have been proposed [9]. These methods have been developed to propagate and concentrate the energy of an ion beam outside the geometric focal plane through a strong magnetic field or wall-confined plasma channel [12–15]. We developed and investigated the method for ion beam transportation in a metal drift tube without the use of additional power sources to ensure the conditions of beam transportation [16]. Experimental studies were performed at TEMP accelerator. To form an intense ion beam we used the ion diode with external magnetic insulation [3]. The design of diode system is schematically shown in Fig.1a.

To obtain geometric focusing of the extracted ion beam, both anode and cathode systems form a portion of cone surfaces. The cathode system consisted of two cathodes and was fixed to the base plate perpendicular to the anode surface. The cathodes were made of stainless steel with a thickness of 0.4 mm. The anode surface had ring grooves which were filled with polyethylene. The dielectric emission coating had an area of 120 cm². The focal plane of the ion beam was located at a 240 mm distance from the anode surface. In our experiments, the distance between the edge of the outer cathode and the anode surface was 7 mm.

In order to reveal the effect of the tube shape on the beam characteristics, we designed several tubes for transportation the annular ion beam. In fact, the drift tube was a hollow stainless steel cone that continued the outer cathode. The tube was installed on the diode base plate as shown in Fig.1a. The length of each tube was 180 mm and corresponded to the position of the focal plane, the wall thickness of the cone was 0.4. The large base of the cone had a constant diameter of 170 mm and the diameter of the small base \varnothing_{SB} varied from 30 to 90 mm.

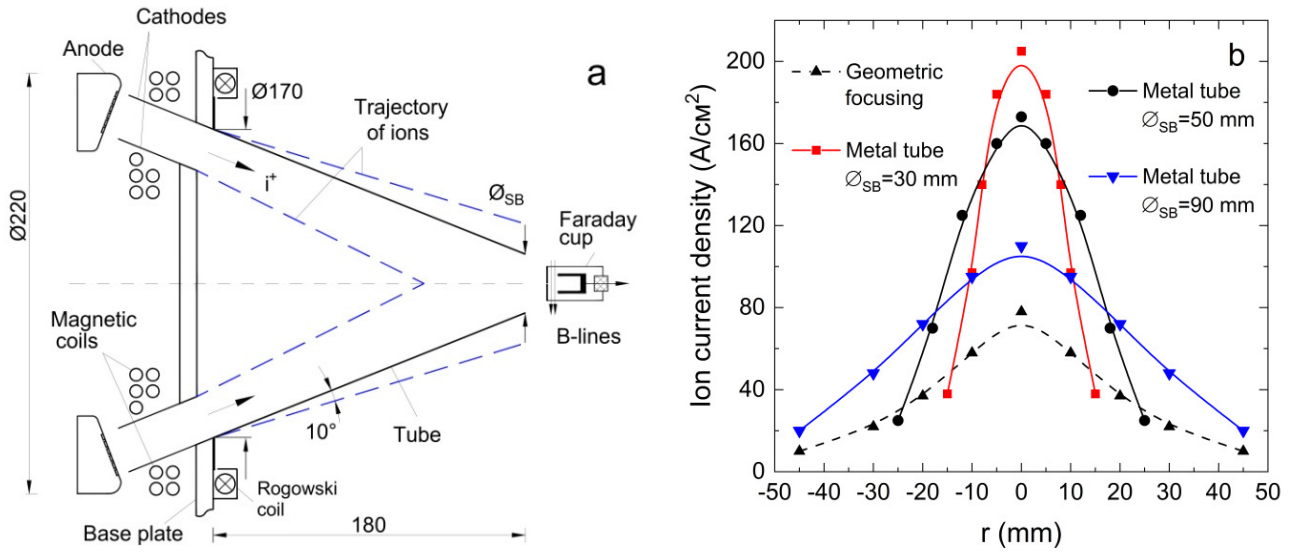


Fig.1. Design of diode system (a), radial distribution of ion current (b).

In this paper, the main attention is paid to the study of the beam characteristics to compare the conditions of its propagation into the metal tube and into outer space (geometrical focusing). The measurements of beam parameters were carried out in the output area of diode and at the distance of 180 mm from the diode base plate (in the focal plane). Using several copper calorimeters, we measured the total beam energy and calculated energy density according to the size of a beam spot. These experimental data were supplemented with the results of ion current measurements using a Rogovski coil.

To find the radial ion current distribution, we used the collimated Faraday cup with magnetic cut-off. It was located on the beam axis and moved along the beam cross section with a step of 5–10 mm. Based on these data, the average ion current I_{IB} in the beam cross section was calculated. The focusing factor K of the beam was estimated as the ratio of the ion current densities measured in the focal plane and near the anode surface.

2. Experimental results

We investigated the ion beam profile in outer space using dosimetric films. The results have shown that the outer and inner boundaries of the beam expanded during the propagation, as shown in Fig.1a. This has increased the total diameter of a beam spot in focal plane up to ~ 90 mm. The resulting angle of a beam divergence was $\sim 10^\circ$, as shown in Fig.1a. The divergence of ions and collision with atoms of residual gas led to a decrease in the beam energy in transport area by 26%, while the ion current decreased from 5 to 3.9 kA (Table 1). In this case, the distribution of ion current density had maximum in the central area of the spot and reached 70 A/cm^2 (Fig.1b), the focusing factor K was equal 4.5.

The process of beam transportation in the tube was accompanied by additional energy and current losses. If the tube angle was less than or equal to the angle of beam divergence ($\sim 10^\circ$), the ion beam flow was directed locally to the inner surface of the tube. Therefore, the tube with the smallest diameter \varnothing_{SB} of small base limited maximally the extracted ion beam flow. As a result, the energy and current of the extracted beam decreased to 20.7 J and 1 kA, respectively (Table 1).

Table 1. Ion beam parameters

Parameter	Geometric focusing	Drift tube $\varnothing_{SB} = 30, \text{ mm}$	Drift tube $\varnothing_{SB} = 50, \text{ mm}$	Drift tube $\varnothing_{SB} = 90, \text{ mm}$
Ion current I_{RC} , kA			5	
Beam energy, J			100	
Ion current I_{IB} , kA	3.9	1	2.5	4.8
Beam energy in focal plane, J	73.8	20.7	46.3	66.4
Beam spot, cm^2	78.5	7.1	19.6	63.5
Energy density, J/cm^2	0.8	2.9	2.4	1
Focusing factor K	4.5	13	11.3	6.5

However, the application of a drift tube significantly improved the conditions of the beam propagation. The ion current distribution presented in Fig.1b has demonstrated an increase in the current density over the beam cross-section. In the central area of spot, the current density reached $205 \text{ A}/\text{cm}^2$, while the factor K grew from 4.5 to 13, as demonstrated Table 1.

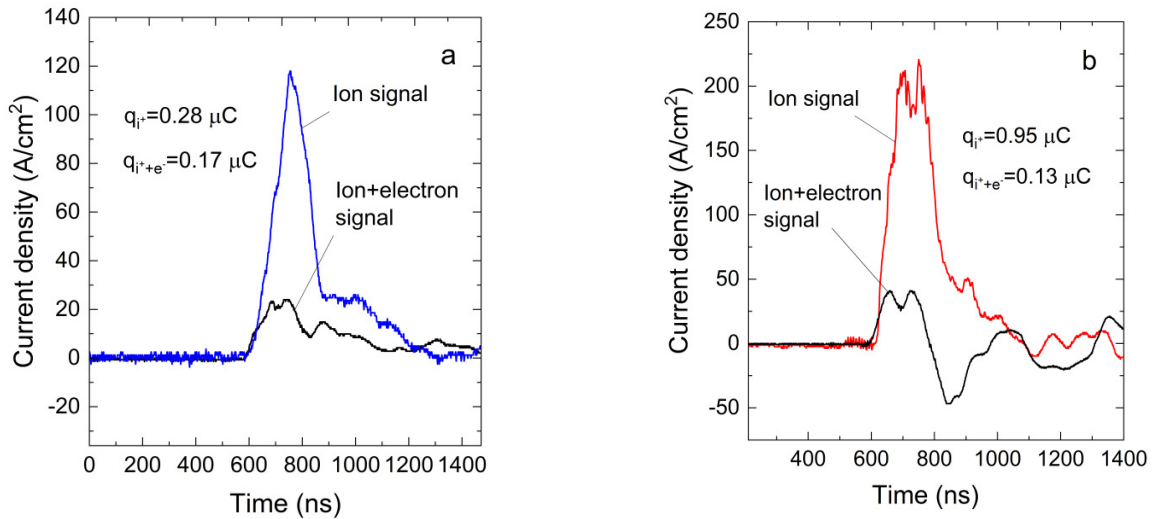


Fig.2. Ion signals: geometric focusing of ion beam (a), ion beam transportation in metal tube $\varnothing_{SB} = 30 \text{ mm}$ (b).

The improvement in the conditions for beam propagation in the drift tube was accompanied by a change in the beam space charge. This means a change in the level of beam charge neutralization. To estimate the coefficient of beam charge neutralization N , we carried out measurements of the ion component and total component (taking into account the ion and electron current) of a beam current using the collimated Faraday cup in the focal plane, as shown in Fig.1a. The total beam current was measured with a Faraday cup without cut-off; in this case the electron and ion current components were closed to the collector. The coefficient of neutralization N was calculated as

$$N = \left(1 - \frac{q_{i^+} + e^-}{q_{i^+}} \right) \cdot 100, \quad (1)$$

where q_{i^+} – charge of ions, $q_{i^+e^-}$ – total charge of ions and electrons. The electrical charge was calculated by integrating the current signals.

Transportation of a beam in the outer space provided only a partial neutralization of the positive beam charge. This is evidenced by the positive value of signals of total current in Fig.2a. In this case, electrons entering in the beam space were formed on the cathodes surfaces as a result of

ion-electron emission, as well as due to ionization of residual gas atoms in the transport region. In this case, the coefficient N was $\sim 38\%$.

The ion flow directed to the inner surface of the tube contributed to the formation of an electron charge as a result of an ion-electron emission. Electrons entered the beam space and neutralized the positive beam charge. The reducing of magnitude of total current signal to zero after 200 ns, as shown in Fig.2b, confirmed the increase in neutralization of beam charge. In this case, the coefficient N rose to $\sim 90\%$.

In addition, we analyzed the form and ion mass spectrum of the beam using the time-of-flight technique, as shown in Fig.3a and Fig.3b. The ion current pulses were recorded simultaneously by two Faraday cups, one of which was located at a distance of 60 mm from the anode surface (in the area of the base plate), and the second one – at a distance of 260 mm on the diode axis.

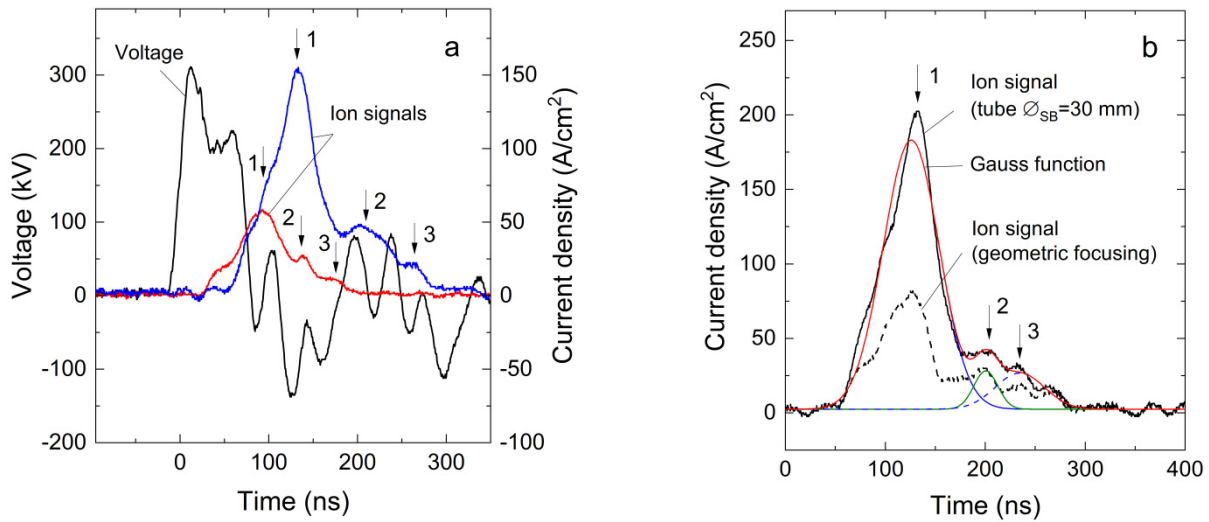


Fig.3. Time-of-flight measurements (a), multiple peak approximation (b).

Registered ion current pulses had a similar waveforms and several peaks, as shown in Fig.3b. The ion peaks were superimposed on each other due to the short time-of-flight base. Therefore, to find the ratio of the mass components, we used the multiple peak approximation by the Gaussian function. We found three distinct peaks (Fig.3b), which is well consistent with the data of the γ -spectrometer [15]. The first peak was identified as the protons H^+ , the second and third peaks – as doubly and singly ionized carbon ions C^{n+} . The ratio of mass components H^+/C^{n+} in geometrically focused beam was 75.7% / 24.3% (Table 2). The mass portion of protons in the beam injected in tube increased to 84.7%. Based on time-of-flight technique, the average speed V_i of the drift motion and the momentum $m_i \cdot V_i$ were evaluated for each ion current component (Table 2).

Table 2. Ion mass spectrum

Parameter	1(H^+)	2(C^{2+})	3(C^+)
Mass ratio (geometric focusing), %	75.7	11	13.3
Mass ratio (drift tube $\varnothing_{SB} = 30$ mm), %	84.7	5.3	10
$V_i \cdot 10^6$ m/s	5.8	2.4	2.1
$m_i \cdot V_i$, kg·m/s	$9.6 \cdot 10^{-21}$	$4.8 \cdot 10^{-20}$	$4.1 \cdot 10^{-20}$

It is clearly seen that an increase in the density of ion current is mainly provided by protons. The intense electric field is generated by the positive charge of the beam of scattered ions. Since the carbon ions had a greater momentum at the same potential energy, the protons left the ion beam

space. Thus, in the drift tube, the electric field of the beam was compensated by the charge of electrons and the scattering of protons decreased.

3. Conclusion

Installation of the cone-shaped metal drift tube on the base plate of the diode provides focusing and neutralization of the ion beam. The focusing factor K depends on the geometric characteristics of the tube and in this study was equal to $K = 13$. In comparison with the geometric focusing, the beam energy loss in the drift tube was higher due to the local flow of ions directed to the inner surface of wall. Nevertheless, the average energy density of the ion beam increased to 2.9 J/cm^2 over the beam cross-section in the focal plane.

Acknowledgments

The reported study was funded by RFBR and NSFC, project number 21-53-53013 and was supported with the State Task in the Field of Scientific Activity FSWW-2020-0008.

This research was supported by TPU development program.

4. References

- [1] Deichuli P.P., Fedorov V.M., *Proc 8th International Conference on High-Power Particle Beams*, Russia, Novosibirsk, 469, 1990.
- [2] Zhu X.P., Lei M.K., Dong Z.H., Ma T.C., *Rev. Sci. Instrum.*, **74**, 47, 2002; doi: 10.1063/1.1529303
- [3] Stepanov A.V., Remnev G.E., *Instrum. Exp. Tech.*, vol. **52**(4), 565, 2009; doi: 10.1134/S0020441209040174
- [4] Zhu X.P., Xu Z.C., Miao S.M., Lei M.K., *Surf. Coat. Technol.*, **201**, 5264, 2007; doi: 10.1016/j.surfcoat.2006.07.142
- [5] Zhu X.P., Ding L., Zhang Q., Isakova Yu., Bondarenko Y., Pushkarev A.I., Lei M.K., *Laser Part. Beams*, **35**, 587, 2017; doi: 10.1017/S026303461700060X
- [6] Stepanov A.V., Shamanin V.I., Remnev G.E., *Rev. Sci. Instrum.*, **90**(3), 033302, 2019; doi: 10.1063/1.5092127
- [7] Yatsui K., Masugata K., Matsui M., *Phys. Rev. A: At. Mol. Opt. Phys.*, **26**, 3044, 1982; doi: 10.1103/PhysRevA.26.3044
- [8] Olson C.L., *J. Fusion Energy*, **1**(4), 309, 1981; doi: 10.1007/BF01050299
- [9] Kaganovich I.D., Davidson R.C., Dorf M.A., Startsev E.A., Sefkow A.B., Lee E.P. Friedman A., *Phys. Plasmas*, **17**, 056703, 2010; doi: 10.1063/1.3335766
- [10] Slutz S.A., Lemke R.W., Pointon T.D., Desjarlais M.P., Johnson D.J., Mehlhorn T.A., Filuk A., Bailey J., *Phys. Plasmas*, **3**(5), 2175, 1996; doi: 10.1063/1.871672
- [11] Petrov A., Polkovnikova N., Tolmacheva V., Matvienko V., Shlapakovski A., *Proc 6th Int. Conf. Modification of Materials with Particle Beams and Plasma Flows*, Tomsk, Russia, 2002;
- [12] Nakagawa Y., Tamotsu E., *J. Appl. Phys.*, **61**, 470, 1987; doi: 10.1063/1.338246
- [13] Yamada T., Masugata K., Yatsui K., Matsui M., *Jpn. J. Appl. Phys., Part 2*, **21**, 699, 1982; doi: 10.1063/1.338246
- [14] Ikehata T., Mase H., Tanabe T., *Nucl. Instrum. Methods Phys. Res., Sect. B*, **37**, 107, 1989; doi: 10.1016/0168-583x(89)90145-6
- [15] Engelko V.I., Giese H., Kuznetsov V.S., Viazmenova G.A., Schalk S., *Tech. Phys.*, **47**, 350, 2002; doi: 10.1134/1.1463126
- [16] Yu X., Zhang S., Stepanov A.V., Shamanin V.I., et al. *Surf. Coat. Technol.*, **384**, 125351, 2020; doi: 10.1016/j.surfcoat.2020.125351

- [17] Stepanov A.V., Haowen Zhong, Zhang Shijian, Mofei Xu, Xiaoyun Le, Remnev G.E., *Vac.*, **198**, 110892, 2022; doi: 10.1016/j.vacuum.2022.110892
- [18] Poukey J.W., Humphries S., *Appl. Phys. Lett.* **33**, 122, 1978; doi: 10.1063/1.90305
- [19] Ryzhkov V.A., Stepanov A.V., Pyatkov I.N., Remnev G.E., *Nucl. Instrum. Methods Phys. Res., Sect. A*, **1013**, 165671, 2021; doi: 10.1016/j.nima.2021.165671